Progress in DNS and Laser Diagnostics of Turbulence and Turbulent Combustion

Mamoru Tanahashi [†], Masayasu Shimura [†], Yuki Minamoto [†]

Abstract

In the community of turbulence and turbulent combustion research, results obtained from direct numerical simulations and advanced laser diagnostics are regarded as forming the fundamental basis of physical insights and mathematical models of the highly non-linear, multi-physical phenomena. Over the decades, we have contributed in these research areas by means of these numerical and experimental approaches, and tried to ellucidate relevant physical mechanisms. The scale of these simulations or laser diagnoctics has improved over the years thanks to the advancement of high performance computing, numerical schemes, and laser and optical systems. The insights based on these numerical and measured resutls are then applied to develop mathematical models to describe microscale non-linear acitivities incorporating theories, which could be used for computational fluid mechanics of major combustion devices.

Key Words: *Turbulence, Turbulent combustion, Direct numerical simulations, Advanced laser diagnostics*

1. INTRODUCTION

The first author of this paper (Mamoru Tanahashi: MT) would like to give a huge thanks to the Heat Transfer Society of Japan for selecting him to be the Nukiyama Memorial award recipient in 2016. The Nukiyama Memorial award has been established in 2012 on the occasion of the 50th anniversary of the foundation of the Heat Transfer Society of Japan. The name of this award has been commemorating great contributions by Professor Shiro Nukiyama who discovered the boiling curve (so-called Nukiyama curve). MT appreciates the international evaluation board by selecting him for this award even though MT's research areas, which are turbulence, turbulent heat/mass transfer and turbulent combustion, are far from the boiling research.

MT makes cordial acknowledgments to Professor Koichi Hishida, Keio University, Japan, Professor Emeritus Godfrey Mungal, Stanford University & Dean at Santa Clara University, USA, Professor Andreas Dreizler, TU Darmstadt, Germany, Professor Sangmin Choi, KAIST, Korea, Professor Yasuyuki Takata, Kyushu University, Japan. Without their strong recommendations, MT were not bestowed this award. MT expresses special thanks to Professor Emeritus Toshio Myauchi, Tokyo Institute of Technology, Japan. MT's research has been initiated by Professor Toshio Miyauchi from the undergraduate research in 1989. He has led that MT should extend direct numerical simulation (DNS) of turbulence to turbulent combustion field in the future. After that, he supervised MT's master and doctoral degrees and has been a senior gentle colleague. MT also appreciate Professor Kunio Hijikata, Tokyo Institute of Technology, Japan who passed away in 1997. He was the supervisor of MT's master degree since Professor Toshio Miyauchi was absent in Japan and he had been encouraged MT as a great professor in the heat transfer society. MT also expresses thanks to also all smart students who had been part of his laboratory and conducted research work extensively, and all friends in this society.

In this paper, MT's research works are summarized with focusing on DNS and laser diagnostics of turbulence and turbulent combustion. In section 2, the pro-

Received: June 30, 2017, Editor : Katsunori Hanamura

[†] Department of Mechanical Engineering, Tokyo Institute of Technology, Ookayma 2-12-1, Meguro-ku, Tokyo 152-8550, Japan

gress in DNS of turbulence and turbulent combustion is discussed. In section 3, recent developments in laser diagnostics of turbulence and turbulent combustion are shown. Finally, in section 4, a short summary is presented.

2. STATE OF THE ART—DIRECT NUMERICAL SIMULATIONS

2.1 Fundamentals of DNS and HPC

The "first principle" numerical simulation method for turbulent flows is called direct numerical simulations (DNS). In this method, Navier-Stokes equations as well as other relevant scalar equations are solved numerically without using a mathematical model except for the chemical source terms if the flow field involves chemically active scalars. The advantage of the use of DNS is that all the fluctuation scales of turbulence and scalars are explicitly resolved both in time and space, thereby naturally including any relevant non-linear fluid flow phenomena. This advantage of DNS is well represented in the study of "coherent fine scale eddies", which determines the structure of smallest eddies prior to their dissipation. Several examples of such smallest eddies are shown in Fig. 1 (Tanahashi et al., 2004a; Wang et al., 2007). Numerical approaches used for many industrial applications, such as Reynolds averaged Navier-Stokes (RANS) or Large Eddy Simulations (LES), are not suitable for this kind of studies since any representation of such small eddies are masked by mathematical models.

While DNS of non-reacting turbulent flows have been already standard method to study fundamental physics of turbulence for around 30 years, direct numerical simulations of turbulent combustion using a single-step chemistry model with variable density have started being used for two- and three-dimensional do-

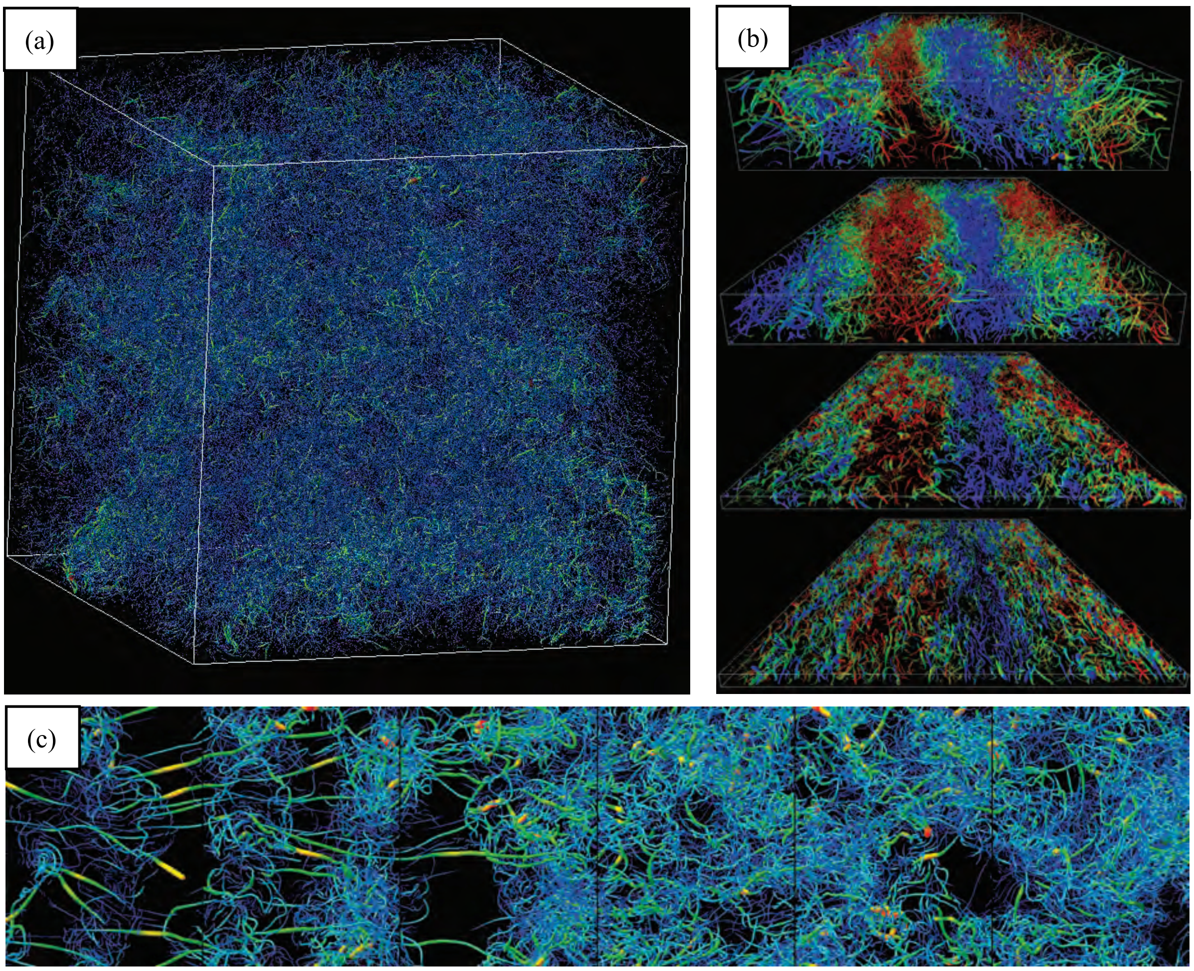

Fig. 1 Typical axis distribution of coherent fine scale eddies in homogeneous isotropic turbulence (a), in a turbulent channel flow (b) and in a turbulent mixing layer (c).

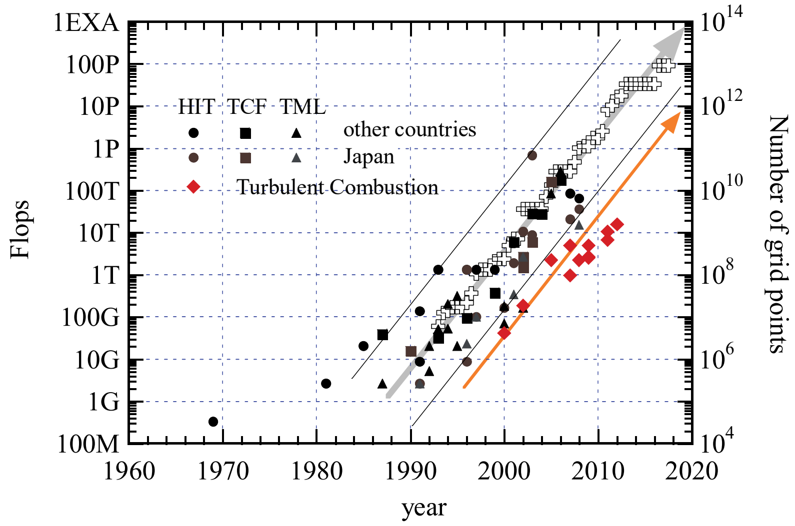

Fig. 2 Development of the fastest supercomputer in the world and grid points of DNS of various turbulence and turbulent combustion.

mains since early 90s. However, as it is well known, assuming single step chemical reaction is indeed oversimplification since the effect of localized radicals and intermediate species on the major species and global flame structure could be substantial during the process of turbulence-flame interaction. The first three-dimensional DNS with a detailed chemistry including all radicals and intermediates including temperature-dependent transport properties has been performed for hydrogen-air premixed combustion at Tokyo Tech and reported in 1999 (Tanahashi et al., 1999; Tanahashi et al., 2000; Tanahashi et al., 2002; Poinsot and Veynante 2005). This has been then followed by many more DNS with complex or detailed chemical kinetics, which are nowadays standard practice in the turbulent combustion research community. This is mostly due to the recent understanding of importance of such chemical kinetics and advancement of high performance computing.

Figure 2 shows a trend of the fastest supercomputer in the world (hereafter, #1 SC) (http://top500.org/). As of June 2017, the #1 SC has about 93 PFlops. The fastest supercomputer in Japan is Oakforest-PACS (about 13.5 PFlops) at Joint Center for Advanced High Performance Computing of the University of Tokyo and Tsukuba University (not K computer). Recent improvement rate of #1 SC is 10 times in 3.5 years. If this rate is sustained, 1 EXAFlops supercomputer will be realized in 2020, where EXA means 10^{18}. In Fig. 2, developments in total grid points used in DNS of nonreactive turbulence are also presented. Here, the plots are split into DNS by Japan and other countries for each fundamental turbulent field (homogeneous isotropic turbulence: HIT, turbulent channel flow: TCF and turbulent mixing layer: TML). The number of grid points used in DNS of turbulence increases at the same rate of the #1 SC. Figure 2 suggests that the K computer will realize DNS of turbulence with 10^{12} grid points. The trends of the #1 SC and DNS also suggest that DNS with 10^{14} grid points is projected to be reported in 2020, if the trend continues.

In numerical simulations of turbulent combustion with complex or detailed chemistry, one need to solve multiple species conservation equations together with mass, momentum and energy conservation equations. The number of species is around 10 for hydrogen and about 50 for methane or propane related combustion. For gasoline, several hundred species should be considered in DNS to include the influence of important chemistry on turbulent combustion. The reaction rate of each species is determined from the complicated pathways of elementary reactions. The number of elementary reactions also depends on fuel: around 30 for hydrogen; around 300 for methane or propane; and several thousand for gasoline. These reaction “layers” need to be explicitly resolved in DNS, and the overall reaction zone thickness is typically much less than 1 mm, within which all of these reaction layers are located at different posi-

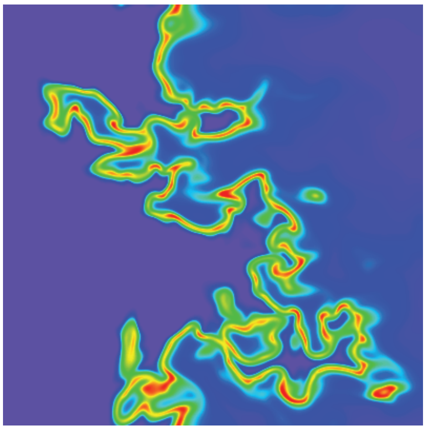

Fig. 3 Distributions of heat release rate in high Reynolds number turbulent premixed flame (Re_λ = 120).

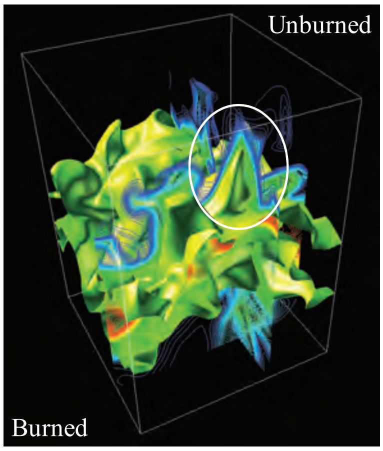

Fig. 4 Radical fingering in high intensity turbulent premixed flame.

tions and variations. To fully resolve flame inner reaction structure, each of these reaction layers need to be resolved by approximately 5-10 mesh points, which easily overwhelms the resolution requirement imposed by Kolmogorov length scale for turbulence. In the next few subsections, we will summarize key combustion DNS performed at our and other groups in the past 30 years

2.2 DNS of High Reynolds Number Turbulent Premixed Flames

From the first 3D DNS of turbulent combustion with a detailed kinetic mechanism, around 20 years has passed. Nowadays, 3D DNS becomes a powerful tool in turbulent combustion research. Similar to the research trend in DNS of non-reacting turbulence, DNS of turbulent combustion is used for investigation of turbulent flame structure which is hardly obtained by experimental studies and development/ validation of turbulent combustion models. However, Reynolds number in DNS is very low compared with that in many combustors in real applications even for state of the art DNS and then DNS at high Reynolds number has been required to understand the turbulent combustion phenomena in real combustors. Figure 3 shows a result of our resent 3D DNS of turbulent premixed flame (Shim et al., 2011). Visualized quantity is heat release rate which is rate of energy conversion to heat from chemical bond. Reynolds number based on Taylor micro scale (Re_λ) of this DNS is about 120. Higher Reynolds number case (Re_λ = 220) is also conducted by using about 1.8 billion grid points. Compared to DNS of non-reaction turbulence, one may feel that the number of grid points of this DNS is not so huge, while this DNS is the highest Reynolds number case for turbulent combustion, as far as we know. Although Reynolds number of turbulent combustion fields in real applications is higher than that of this DNS and seems to be higher than Re_λ =300, more than 10 years are required for the realization of such kinds of DNS. Note that actual Reynolds number in real combustors is not known because detailed experimental data are not enough.

In the above paragraph, the expression of ‘high Reynolds number’ is used to represent turbulent combustion phenomena. However, this expression is not always appropriate to characterize the turbulent combustion because that consists of two phenomena: turbulence and flame, and both of them have independent representative scales. Reynolds number only represents physical state of turbulence side. Even for the same Reynolds number, if the characteristic scale ratios of two phenomena are different, characteristics of turbulent flame are significantly affected. It should be noted that the product of velocity scale ratio (u'_{rms}/S_L) and length scale ratio (l/δ_F) represents Reynolds number based on the integral length scale. For the cases in which velocity scale ratio is high, we call this state ‘high intensity turbulent premixed flames’. Since these flames are hardly attained in laboratory scale burners and measurements in this condition is quite difficult, detailed flame structures have not been clarified.

In Fig. 4, one example of DNS of high intensity hydrogen-air turbulent premixed flame is shown (Shim et

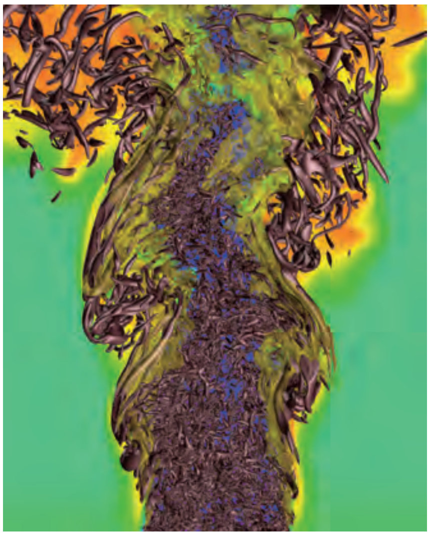

Fig. 5 DNS of turbulent jet premixed flame (Re_λ = 97.1). Instantaneous contour surfaces of temperature (T = 1400 K, clear yellow) and eddies (bronze), and distribution of OH mole fraction on a typical *x*-*y* plane.

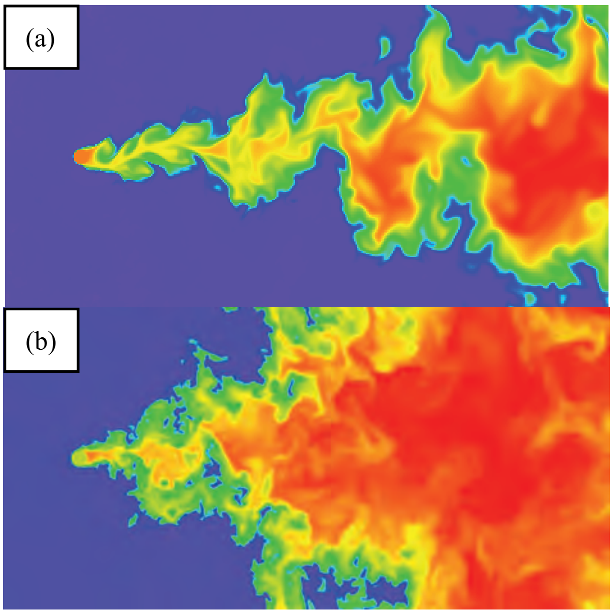

Fig. 6 Pressure effects on flame structure in turbulent V-shape premixed flame. Distributions of temperature at (a) 0.1 MPa, (b) 0.2 MPa.

al., 2013). In this condition, since time scale of elementary reaction and that of coherent fine scale eddies becomes in comparable order, inner structure of local flame elements reflects effects of turbulent motion and shows particular behaviors. In Fig. 4, concentration of one important radical, HO_2, which is shortly created in the process of hydrogen combustion, is presented. In laminar flame, this radical is created in front of thin flame surface (unburned side). In high intensity turbulent flames, however, that is transported in low temperature regions where that radical hardly exists in general condition by the strong turbulent motion. The authors called this phenomenon as 'radical fingering'.

2.3 DNS of Turbulent Premixed Flames in Complex Geometry

Recent DNS of turbulent combustion has been extended to relatively complex combustion geometry such as jet flames (Sankaran et al., 2007; Bell et al., 2007; Hawkes et al., 2009; Shimura et al., 2012), V-shape flames (Bell et al., 2005; Minamoto et al., 2011; Fukushima et al., 2013), swirling flames (Tanaka et al., 2011; Luo et al., 2011; Wang et al., 2011; Aoki et al., 2014; Minamoto et al., 2015), flame propagation in a constant volume vessel (Yenergdag et al., 2014), etc. Figure 5 shows an example of DNS of turbulent jet premixed flame (Shimura et al., 2012). In this case, flame is susained by surrounding burnt gas. In this geometry, since velocity difference between unburnt mixture and burnt gas makes mean shear, flame structures are affected both by the mean shear and turbulence, and their statistical nature is very important for the developments in turbulent combustion models used in numerical analyses of real combustors.

In addition to the geometry of combustion fields, pressure effects should be overcome in DNS of turbulent combustion to clarify characteristics of turbulent flames in engineering applications. In general, combustors in real applications are operated at several tens of atm (or several MPa). However, most of turbulent combustion DNS have been conducted at atmosphere pressure condition (0.1 MPa). In high pressure conditions, Reynolds number of the flow field further increases due to the decrease of kinematic viscosity. Pressure effects appear not only in flow fields but also in flame structures. For the flame side, flame thickness at the high pressure becomes thinner even for the same fuel, which results in an increase of grid points in DNS compared to the condition of 0.1 MPa. From these reasons, DNS at high pressure conditions have been difficult. In Fig. 6, temperature distributions obtained from DNS of turbulent V-shape flame at different pressures are shown on a typical cross

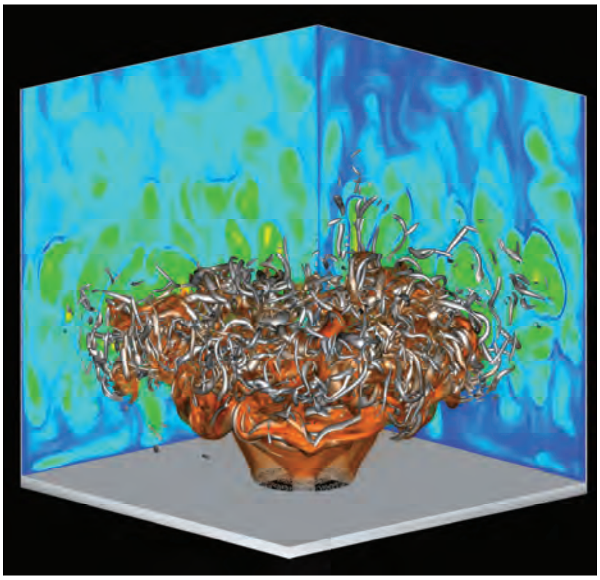

Fig. 7 DNS of turbulent swirling premixed flame in a cuboid combustor. Eddy structures are visualized by contour surface of the second invariant of velocity gradient tensor (gray). Volume rendered heat release rate is shown in orange region. Heat flux on side walls are shown by the rainbow color map.

section. In Fig. 6 (a), temperature distribution for 0.1 MPa (Minamoto et al., 2011) is shown. In Fig. 6 (b), that for 0.2 MPa (Fukushima et al., 2013) is presented for comparison. DNS at 0.2 MPa is just running by using about 1.5 billion grid points which is 3.4 times larger than those of DNS at 0.1 MPa. Only from the increase of grid points, one may understand the difficulty of DNS at high pressure conditions. In these cases, flame is sustained by a high-temperature rod and V-shape flame is created behind the rod. Figure 6 suggests that turbulence-flame interactions strongly depend on the pressure, and those induce complicity in turbulent flame structures. It should be noted that more detailed investigations will be needed to clarify the turbulent flame structures at high pressure conditions.

In a lot of gas-turbine combustors, swirling flow is utilized for flame stabilization. To clarify characteristics of flow and flame structures in gas-turbine like combustors, DNS of turbulent swirling premixed flames in a cuboid combustor has been conducted (Tanaka et al., 2011). Figure 7 shows an example of the DNS with swirl number of 1.2. Swirling flow generates large-scale helical vortical structures in the vicinity of inlet and fine scale eddies develops in downstream region. These vortical motions distort flame geometry, and results in spatial fluctuations of heat release rate. Furthermore, DNS of turbulent flame in a combustor enable us to analyze heat loss from wall, which is significant information for improvement of thermal efficiency of combustors. These sorts of physical quantities are influenced by pressure oscillation in the combustor. From the DNS of turbulent flame in the cuboid combustor, relations between acoustic field and heat release rate in three dimensions can be revealed (Aoki et al., 2014), which will be beneficial to understand experimental data on pressure fluctuations and heat release rate in lower dimensions.

Ignition and flame propagation mechanism are keys for development of high efficiency spark ignition engines. Figure 8 shows examples of DNS of flame propagation in a confined vessel (Yenerdag et al., 2014). Flame is ignited by a hot spot at the center of the vessel and propagates in isotropic turbulence. Flame front is distorted by the turbulence motion and the flame wrinkling increases with increase of pressure in confined vessel. This DNS will contribute to the clarifications of effects of fine scale eddies in turbulence on ignition and flame propagations, pressure effects on flame propagation in turbulence, and flame-wall interactions.

These simulated DNS data sets are very useful to elucidate underlying physics of turbulent combustion, as they include all the relevant information. Also, these data bases are extensively used for the development of mathematical models that describe the non-linear phenomena without explicitly resolving all the scales (Minamoto et al., 2015; Hiraoka et al., 2016a; Hiraoka et al., 2016b).

2.4 New Extensions of DNS of Turbulent Combustion

Recently, as a new extension of DNS of turbulent combustion, many research works have been reported about the investigation of HCCI (homogeneous charge compression ignition) combustion. Since HCCI combustion has an instinct nature of low emission and high efficiency, this will be one of promising combustion technology applying in gas engines in local power generation system and in IC engines for automobiles. However, difficulties in the control of ignition prevent the engi

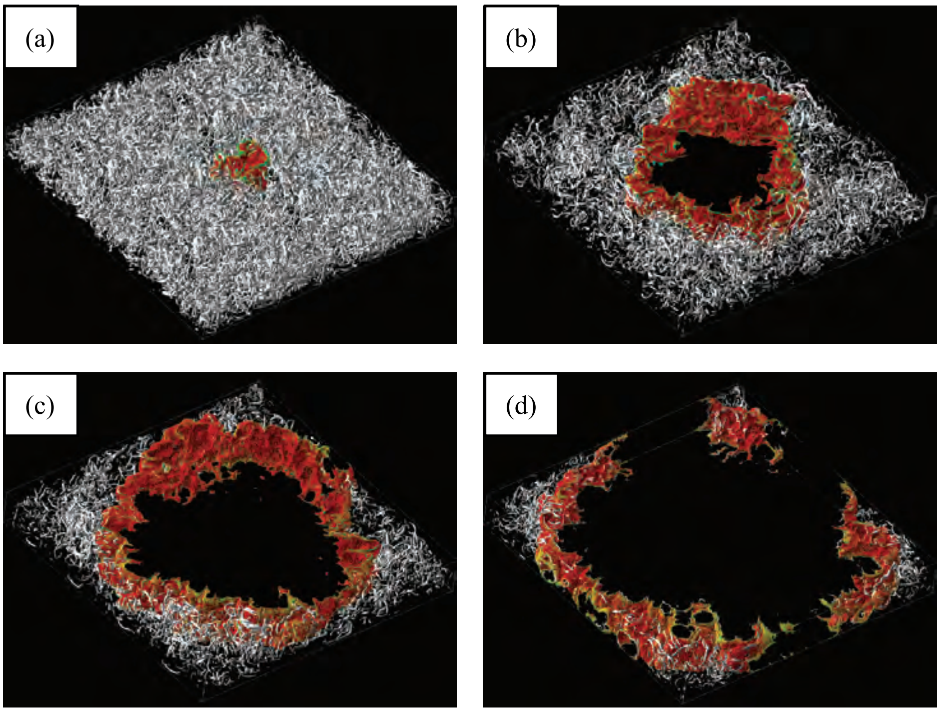

Fig. 8 Temporal development of the local heat release rate at the flame front (orange-red) and turbulent vortices (gray) in the confined volume vessel. (a) t = 97.2 μs, (b) t = 264 μs, (c) t = 360 μs, (d) t = 456 μs.

neering applications of HCCI. To understand HCCI combustion mechanism, DNS of HCCI combustion has been conducted (Chen et al., 2006; Fukumoto et al., 2011; Yoo et al., 2013; Zhang et al., 2013). Figure 9 shows a result obtained from DNS of HCCI turbulent combustion (Fukushima et al., 2014). In this DNS, methane-air mixture is used for fuel and a detailed kinetic mechanism with 53 species and 325 elementary reactions are considered. The pressure condition is about 50 atm which is near those in real applications. In HCCI engines, premixed gas is compressed rapidly up to very high pressure and auto-ignition is enhanced. To reduce drastic pressure raise due to auto-ignition, fluctuations of temperature or equivalence ratio are introduced in general. However, real feature of HCCI combustion with temperature or mixture fluctuations has not been clarified yet. To investigate local combustion characteristics in HCCI condition, Lagrangian particle tracking have been conducted with DNS of flow and combustion field. From temporal development of physical and chemical quantities on a particle, combustion regimes depending on local temperature and mixture condition at the initial stage have been clarified. This DNS is still limited in two-dimension, while this will be extended for 3D in the near future.

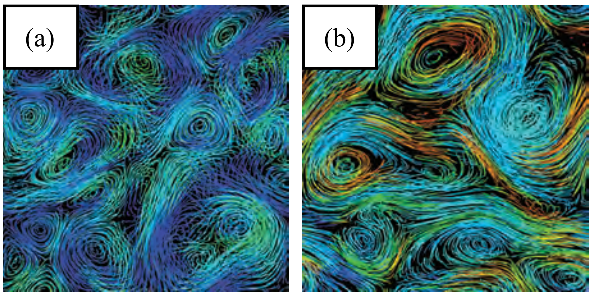

Fig. 9 DNS of HCCI turbulent combustion. Examples of results of fluid particle tracking analysis t = 0 μs - 60 μs (a) and 300 μs - 360 μs (b). Red and blue show high and low temperature.

For the distributed power generation system and portable power generation, micro combustion technology is in the spotlight. Although combustion phenomena in micro combustors are in laminar state in general, detailed information obtained from DNS gives great impacts on understanding of the micro combustion. The application of DNS to micro flow reactor (Miyata et al, 2015) is one typical example.

2.5 Projection of Turbulent Combustion DNS

To show the possibility of the perfect simulation of internal combustion engines, a trend for gird points used in DNS of turbulent combustion is shown in Fig. 2. DNS of turbulent combustion plotted in Fig. 2 have been conducted for hydrogen fuel with a detailed kinetic mechanism including 12 reactive species and 27 elementary reactions. From the estimation in Sec. 2.1, required memory is about 5×10^3 times that for incompressible turbulence. Figure 2 shows that the number of grid points used in DNS of turbulent combustion is lower than that of turbulence with this factor. The increasing rate of the grid points used in DNS of turbulent combustion also coincides with that of #1 SC similar to DNS of turbulence. If the K computer is used, 10^{10} gird points will be used for DNS of turbulent combustion. For 1 EXA Flops, that with 10^{12} will be reported in 2020. Here, it should be noted that this expectation is for hydrogen fuel. In many combustors in engineering applications, hydrocarbon fuels are used. As for heptane which is one composition of gasoline, a detailed kinetic mechanism will be constructed from 544 reactive species and 2446 elementary reactions. In this case, the number of available grid points is reduced to about 30 billion (3100^3) due to increase in required memory. Here, based on the first three-dimensional DNS of turbulent combustion, CPU time which is required for DNS of a cylinder of an automobile IC engine (1600 cc) can be estimated. Even for the present #1 SC which has 93 PFlops, 3 years are required for the perfect simulation of IC engine. If the 1 EXAFlops SC is realized, this CPU time is reduced to about 4 months. This estimation suggests that DNS of IC engines is possible in 2020.

To shorten CPU time required for DNS of turbulent combustion, two numerical methods are introduced to full-explicit full-compressible DNS code. One is compact finite difference filter to reduce spatial resolution requirements and to eliminate higher spatial frequency oscillations than the spatial resolution, and another is well-known point-implicit scheme to avoid quite small time integration of the order of nanosecond for fully explicit DNS. Availability and accuracy of these numerical methods have been confirmed carefully for auto-ignition, planar laminar flame and turbulent premixed flames (not shown here). These modifications reduce the CPU time

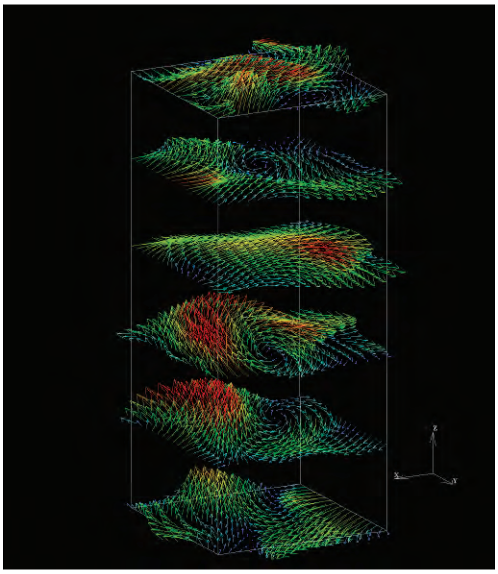

Fig. 10 One of the typical time-series velocity vector distribution images obtained by the time-resolved PIV system (Tanahashi et al., 2004b)

to 5 weeks. In addition to these numerical aspects, physical investigations are required for Soret effect, Dufour effect, pressure gradient diffusion, wall-flame interaction, radiation heat transfer, etc.

Even though the full simulation of IC engine is projected to be realized in 2020, those of large scale combustors such as gas turbine in power generation plant are still impossible. Therefore, for accurate numerical predictions of combustion phenomena in engineering applications, high-accuracy turbulent combustion models should be developed by including many turbulent combustion mechanisms.

3. STATE OF THE ART—LASER DIAGNOSTICS OF TURBULENCE AND TURBULENT COMBUSTION

3.1 Fundamentals of Particle Image Velocimetry (PIV) and Direct Comparison with DNS

Coherent fine scale eddies are investigated and their statistical characteristics are found to be independent of the Reynolds number and flow geometry in previous DNS studies (Jimenez et al., 1993, Tanahashi et al., 1997, Tanahashi et al., 2001, Tanahashi et al., 2004a, Alamo et al., 2006, Wang et al., 2007). The diameter and the

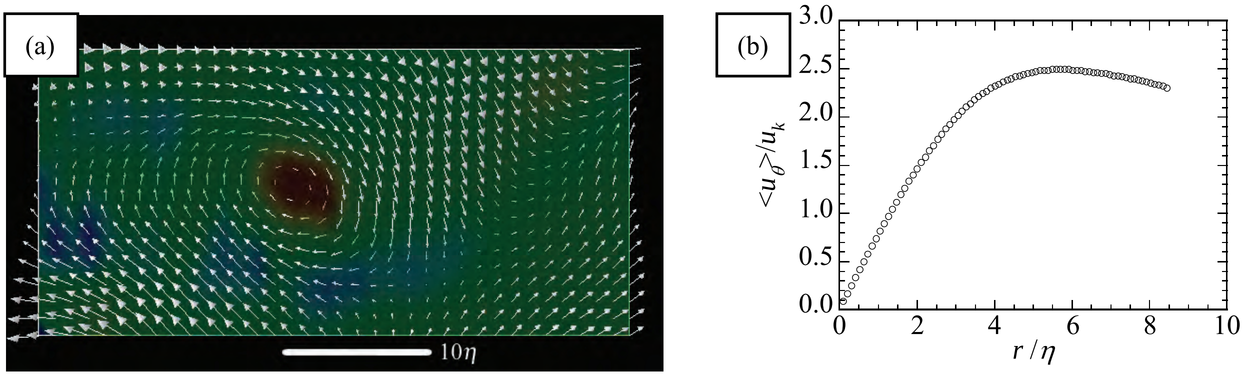

Fig. 11 Distribution of second invariant and velocity vectors around the typical fine scale eddy (a) and mean azimuthal velocity profile of the typical fine scale eddy (b).

maximum azimuthal velocity of coherent fine scale eddies are scaled by the Kolmogorov length (η) and the Kolmogorov velocity (u_k). The most expected diameter and maximum azimuthal velocity are close to 8η and $1.2u_k$ except very near the wall (Tanahashi et al., 2004a). Moreover, these fine scale eddies travel with the velocity of the order of the velocity fluctuation u'_{rms}, and the azimuthal velocity of an intense fine scale eddy can reach up to 3 - 4 u'_{rms}. To investigate the coherent fine scale eddies, high spatial resolution time-series PIV system, of which time-resolution is potentially applicable from several hundreds of Hz to several tens of kHz, has been developed.

To investigate the coherent fine scale eddies, time-resolved stereoscopic PIV system, of which time-resolution is potentially applicable from several hundreds of Hz to several tens of kHz, has been developed. The developed system was applied to flow field of a turbulent jet and fluid flow maps with about 2 kHz time-resolution were demonstrated (Tanahashi et al., 2004b). Figure 10 shows one of the typical time-series velocity vectors images obtained by the PIV system. In addition, measurements with various time-resolution up to 26.7 kHz were also conducted to estimate the performance of the developed high spatial resolution time-series PIV system (Tanahashi et al., 2004b). From the time-series PIV measurement with high temporal and spatial resolution, dynamics of the turbulent structure were visualized clearly. This PIV system was extended to dual-plane measurement by utilizing the difference of polarization of lasers (Tanahashi et al., 2008a). The time-resolved dual-plane stereoscopic PIV was applied to the turbulent jet flow. Figure 11(a) shows distribution of second invariant and velocity vectors around a typical fine scale eddy. The velocity at the center of the eddy is subtracted from the velocity field, and the color represents the second invariant. Here, white represents positive Q and black does negative one. The angle between the vorticity vector at the center of the eddy and the measurement planes is 87.3 degrees. The asymmetric characteristic of the fine scale eddy shown in Fig. 11(a) agrees well with that obtained from DNS (Kang et al., 2006). Figure 11(b) shows mean azimuthal velocity profile of the typical fine scale eddy. The radius and the mean azimuthal velocity in Fig. 11(b) are normalized by η and u_k which are obtained from the present PIV. The radius of the fine scale eddy is defined as the distance between the center and the locations where the mean azimuthal velocity shows the maximum or minimum value. Thus, the diameter of this eddy is 11.4η and the maximum azimuthal velocity $u_{\theta,\max}$ is 2.5 u_k.

3.2 Quad-plane Stereoscopic PIV

The dual plane stereoscopic PIV was used to investigate characteristics of turbulent eddies in a lot of studies. Actually there is a disadvantage in evaluation of velocity gradients in the out-of-plane direction. Although DPSPIV extends the velocity distribution in another dimension, the number of data points in the third dimension is inherently limited in two. Moreover, the computation of the out-of-plane velocity gradient is restricted to 2nd order scheme, and the spatial resolution of the velocity and velocity gradient are determined by the laser light sheet thickness. Recently, the tomographic PIV

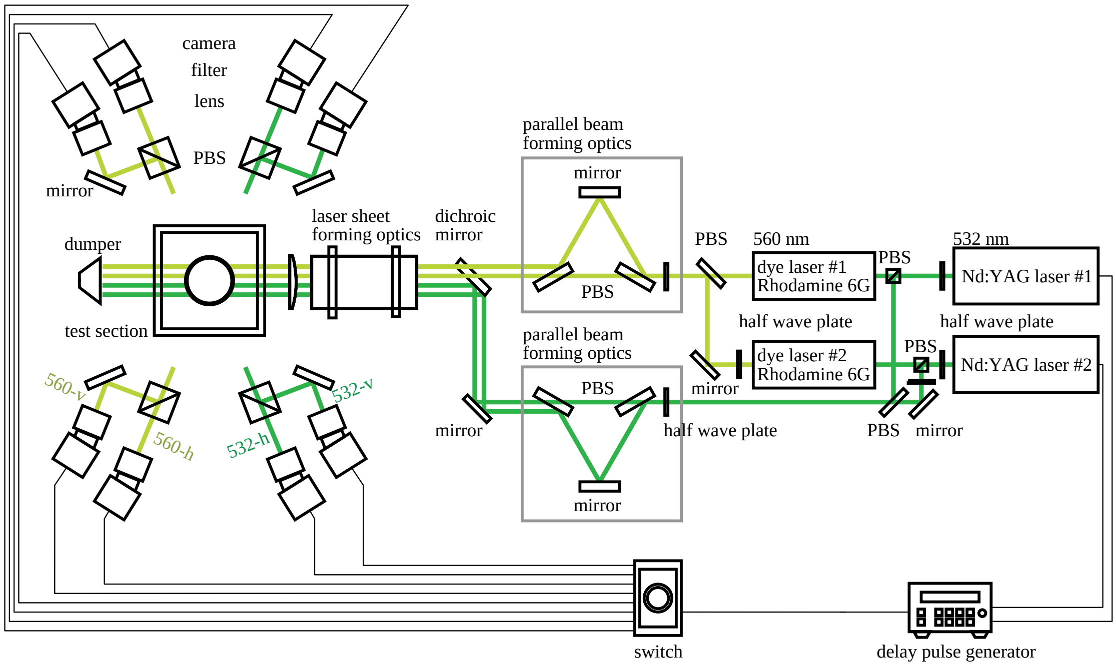

Fig. 12 Schematic of the quad-plane stereoscopic PIV system.

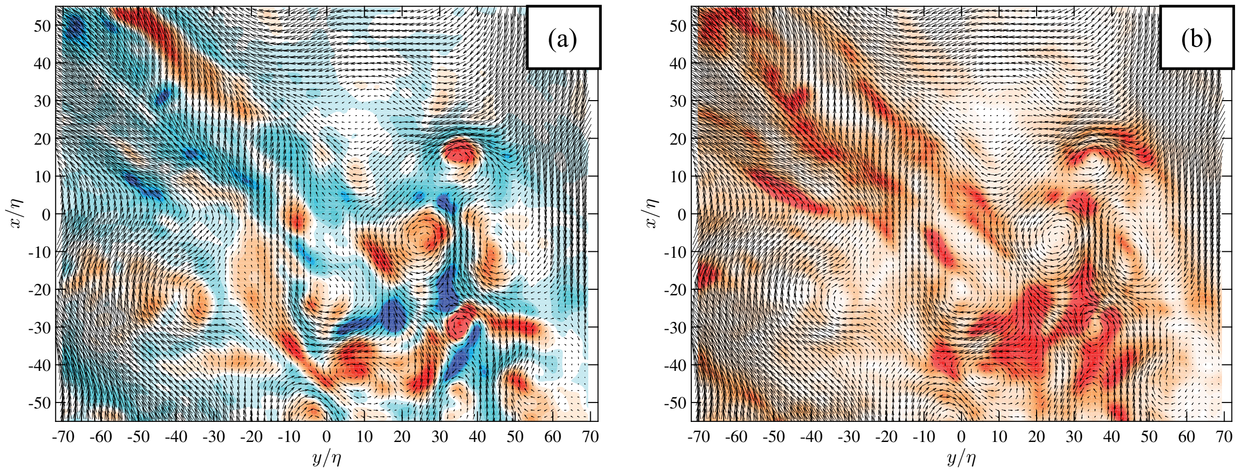

Fig. 13 Instantaneous snapshots of Q (a) and ε (b) on the mid-plane at $Re_\lambda = 128.9$; corresponding in-plane velocity vectors are superposed. The every other velocity vectors are presented for readability: the visualized vector spacing is 1.7η.

technique, which provides 3D3C (three dimensional, three component) velocity field in the measurement volume, has been attracting attention for almost one decade, whereas the spatial resolution is limited mainly by the particle concentration: increasing the number of particles included in one voxel generally ameliorates the quality of cross correlation, but excessive particle concentration would cause ghost particles which are a main source of error of this technique. The ghost particles can be reduced by adding extra cameras eliminating the ambiguity of the particle position, but it requires further particle 3D reconstruction which is computationally exhaustive. For these reasons, higher accuracy in calculating the full velocity gradient tensor is desired for turbulence measurements under high Reynolds number conditions. Hence, quad-plane stereoscopic PIV (QPSPIV) has been developed in our recent study (Naka et al., 2016).

The QPSPIV is accomplished by the difference of laser wavelengths and polarizations. A schematic of the present QPSPIV system is shown in Fig. 12, and its description can be found in the literature (Naka et al., 2016). The advantages of the QPSPIV especially in the effect of the order of the finite difference schemes in the out-of-plane direction was confirmed by resampling the velocity data in-plane directions so that the distance of the data points becomes comparable to the distance of the light sheets which roughly corresponds to the 0% overlap. This can mimic the velocity distributions in the out-of-plane direction, and is effective to check the spectral response.

Measurements were undertaken in the developed region of the turbulent jet with a spatial resolution sufficient to capture the small scale structures. Figure 13 shows the 2D field of Q and ε on the middle plane at Re_λ =128.9. The axes x and y are normalized by η. The pattern of the velocity vector looks to represent some packets of swirling motions. The distribution of Q becomes positive near the center of such rotating motions. On the other hand, ε takes relatively large value slightly off from the center. It is noted that every other velocity vector is displayed for readability: the visualized vector spacing is 1.7η. From these visualizations, it is fair to say that the fine scale structures are well resolved and the size of the measurement area is enough to have several units of such structures in the present measurements. From the high spatial resolution multi-plane PIV enables us to evaluate characteristics of the fine scale eddies in turbulence in comparison with DNS. The QPSPIV can be applied to various flow fields and to the higher Reynolds number conditions.

3.3 Fundamentals of PIV and Planar Laser Induced Fluorescence (PLIF)

As denoted in Sec. 2, characteristics of the turbulent premixed flames are investigated extensively in the recent 3D DNS, and local flame structures which differ from theoretical classifications have been clarified. 3D flame structures, which are caused by strong fine scale eddies in turbulence and described as the handgrip, spire structures and radical fingerings, appear even in the corrugated flamelets regime of the combustion diagram, and enhance flame wrinkling and local heat release rate. The importance of these structures should be investigated by the experiments, while there are a few experimental techniques which have high accuracy enough to compare with DNS. In this section, the progress of laser diagnostics for understanding turbulent combustion mechanism is presented.

To investigate turbulent flame structures experimentally, planar laser induced fluorescence (PLIF) of molecules and radicals produced by chemical reactions such as OH, CO, CH and CH_2O are commonly used. Since OH radicals show high concentration in the burned gas, OH PLIF is useful to distinguish the burned gas from the unburned mixture. Although the edges of OH radical distribution may correspond to the flame fronts for low Reynolds number turbulent flames, there is a possibility that flame fronts do not exist at the edge of OH radicals in high Reynolds number cases in which flame front is significantly distorted and multiply folded. On the other hand, CH PLIF has been used to investigate characteristics of the flame front in turbulence because CH radicals are produced at the flame front and have very narrow width enough to represent the reaction zones. However, it is hard to distinguish the unburned gases from burned gases only from the CH PLIF. To overcome these defects in single radical PLIF, simultaneous PLIF for multi-species, such as OH and CH (Donbar et al., 2000), has been required. In addition to the PLIF measurement, particle image velocimetry (PIV) has been adopted to measure turbulence characteristics near the flame (Donbar et al., 2001). To obtain the detailed information about turbulent velocity field, 3C velocity measurement such as a stereoscopic PIV is desirable.

Figure 14 shows schematic of the measurement system of simultaneous CH-OH PLIF and stereoscopic PIV measurement (Tanahashi et al., 2005) to clarify relation between local flame structure and turbulence characteristics in turbulent premixed flames. Figure 15 shows example of measured CH and OH distributions and 3C velocity map obtained in turbulent methane-air premixed flames on a model swirling combustor of gas turbine. The area denoted by a white box in the CH and OH images corresponds to the measurement region of the stereoscopic PIV. In CH and OH images, red color represents high concentration. In the velocity map, the x and y components are shown by arrows and the z component is represented by color. The velocity from behind to front has positive value and is denoted by red. Flame fronts have large-scale wrinkling of the order of the integral

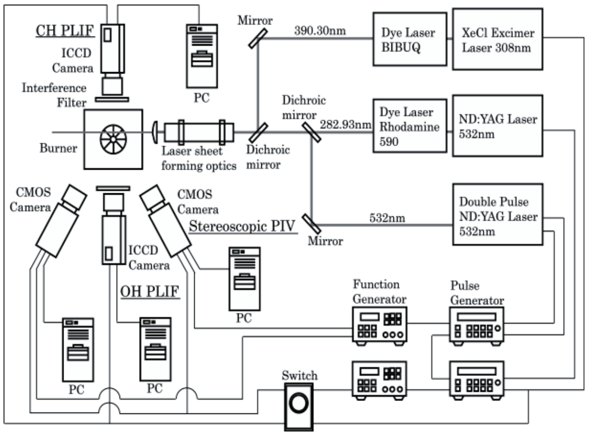

Fig.14 Schematic of simultaneous OH-CH PLIF and stereoscopic PIV system.

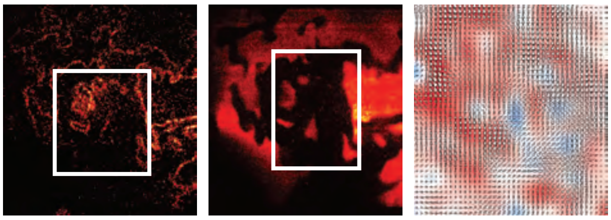

Fig. 15 CH (left) and OH (center) fluorescence images and three-component velocity map (right) (Re_λ = 115.0, ϕ = 1.0).

length scale and small-scale wrinkling less than the Taylor micro scale. By detecting flame front from CH PLIF image and estimating a unit vector normal to the flame front from the gradients of OH at the flame front, flame curvature can be obtained experimentally. Furthermore, from the 3C velocity vector, strain rate acting on the flame surfaces can be evaluated. Since behavior of local flame elements is discussed based on the flame curvature and tangential strain theoretically, this kind of combined laser diagnostics is very important to investigate turbulent combustion mechanism. Noted that, even in this combined laser diagnostics, analyses are limited in two dimensions.

3.4 Multi-dimensional/Multi-variables PLIF and PIV in Turbulent Combustion

The above mentioned combined laser diagnostics have been limited to measure two-dimensional behaviors of turbulent premixed flames. To evaluate flame curvature and tangential strain rates exactly, 3D measurements of turbulent flame are required. Crossed-plane PLIF (Knaus and Gouldin 2000) and multi-parallel-plane PLIF

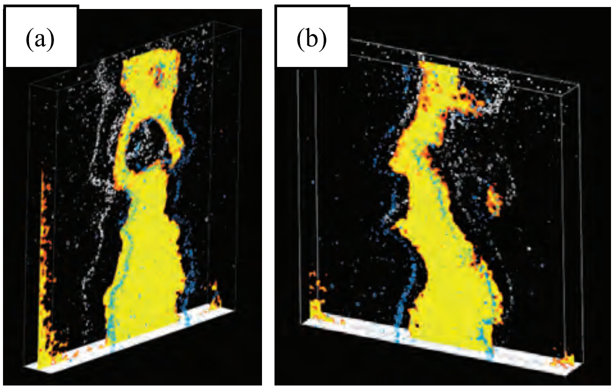

Fig. 16 Typical three-dimensional flame structure obtained by triple-plane PLIF. (a) and (b) represent different realizations.

(Ueda et al., 2009) are useful to achieve the objectives. Figure 16 shows examples of 3D measurements of flame surfaces by a triple-plane PLIF (Ueda et al., 2009). The isolines drawn by blue and white represent fluorescence intensity distributions of CH radicals in each plane, and the yellow area represents the unburned mixture obtained by fluorescence intensity distribution of OH radicals. The visualized distance between two measured planes is twenty times the real scale for easy understanding. By using the multi-plane PLIF, two principal curvatures obtained and curvature terms in the flame stretch concept will be evaluated.

Moreover, to investigate effect of tangential strain rate simultaneously, dual-plane CH planar laser induced fluorescence (PLIF), single-plane OH PLIF and dual-plane stereoscopic particle image velocimetry (PIV) measurement has been developed. This simultaneous measurement can provide three-dimensional flame front, three velocity components and nine velocity derivatives. Details can be found in the literature (Shimura et al., 2011). Dual-plane stereoscopic PIV realizes simultaneous measurement of 3 velocity components and 9 velocity gradients, which gives strain rate exactly without any assumptions. Since flame normal direction can be evaluated from the OH distribution, strain rate tangential to the flame surface can be obtained. Hence, this method is one of promising methods to investigate flame-turbulence interactions.

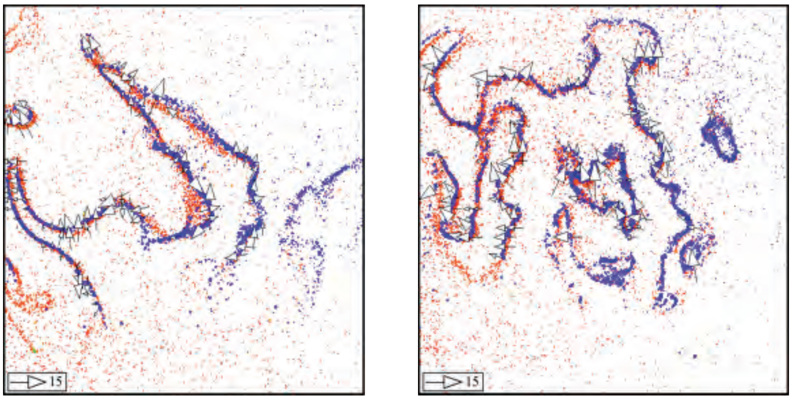

Fig.17 Local flame displacement speed obtained from double-pulsed CH PLIF. Red: 1st shot, blue: 2nd shot, vectors: local flame displacement speed.

3.5 Insight into Dynamics of Turbulent Flames with High Temporal Resolution PIV and PLIF

Dynamics of turbulence and flame affects turbulent flame structures, and high repetition rate PLIF and PIV measurements are significant to understand turbulent combustion mechanism. In the concept of the flame stretch, increasing rate of the flame area is expressed by flame displacement speed, flame curvature and strain rate at the flame front. To confirm the flame stretch concept experimentally, measurements of the flame displacement speed are necessary. For this purpose, time-resolved OH PLIF has been developed (Kaminski et al., 1999). CH double-pulsed PLIF, which was originally developed for study on stabilization mechanism of turbulent non-premixed jet flame (Schefer et al., 1994; Watson et al., 2002), has been utilized to evaluate flame displacement speed in turbulent premixed flames (Tanahashi et al., 2008b). Figure 17 shows vector map of flame displacement speed with successive CH fluorescence images. In these figures, red and blue color represents 1st and 2nd CH fluorescence image, respectively. White vectors represent local flame displacement speed. Directions of flame displacement vectors coincide very well with observations from successive CH fluorescence images. Detailed analyses of this experimental result suggest that theoretical conventional model might be modified. If the CH double-pulsed PLIF is conducted with a stereoscopic PIV simultaneously (Tanahashi et al., 2008c), direct measurement of local burning velocity is possible, and direct validation of the concept of the flame stretch will be realized.

Recently technologies for high speed visualization has been significantly developed. Consequently high-repetition-rate PLIF and PIV measurements have got to have potential to investigate the dynamics of turbulent flames. The high-repetition-rate dual-plane OH PLIF and stereoscopic PIV has been developed and used for investigation on local turbulent displacement speed (Trunk et al., 2013, Peterson et al., 2015). In our previous work, a high-repetition-rate simultaneous measurement of CH–OH PLIF and stereoscopic PIV has been developed (Johchi et al., 2015). The high-repetition-rate simultaneous measurement system has an acquisition rate of 10 kHz and its measurement duration time exceeds 1.0 s.

The developed system was applied to the methane–air turbulent jet premixed flame in order to investigate the flame and flow dynamics of the turbulent combustion field. Examples of the representative PLIF images and distributions of fluctuating velocity acquired by this system are shown in Fig. 18. The illustrated area is approximately 13 mm × 13 mm. The quantized light intensity in the OH and CH images was mapped from 0 (minimum) to 1 (maximum), and the color scale in Fig. 18 is adjusted to better represent the instantaneous distributions. The arrows and background indicate the in-plane (x and y) and out-of-plane (z) component of the velocity fluctuation, respectively. The mean velocity distribution obtained from 10,000 samples was subtracted from the instantaneous velocity. The continuous flame shape at U_0 = 10 m/s (result not shown) turns to exhibit complicated geometry with several flame wrinkles at U_0 = 15 m/s (Fig. 18). Due to the entrainment of burned gas in the unburned region, flame front sometimes appears to

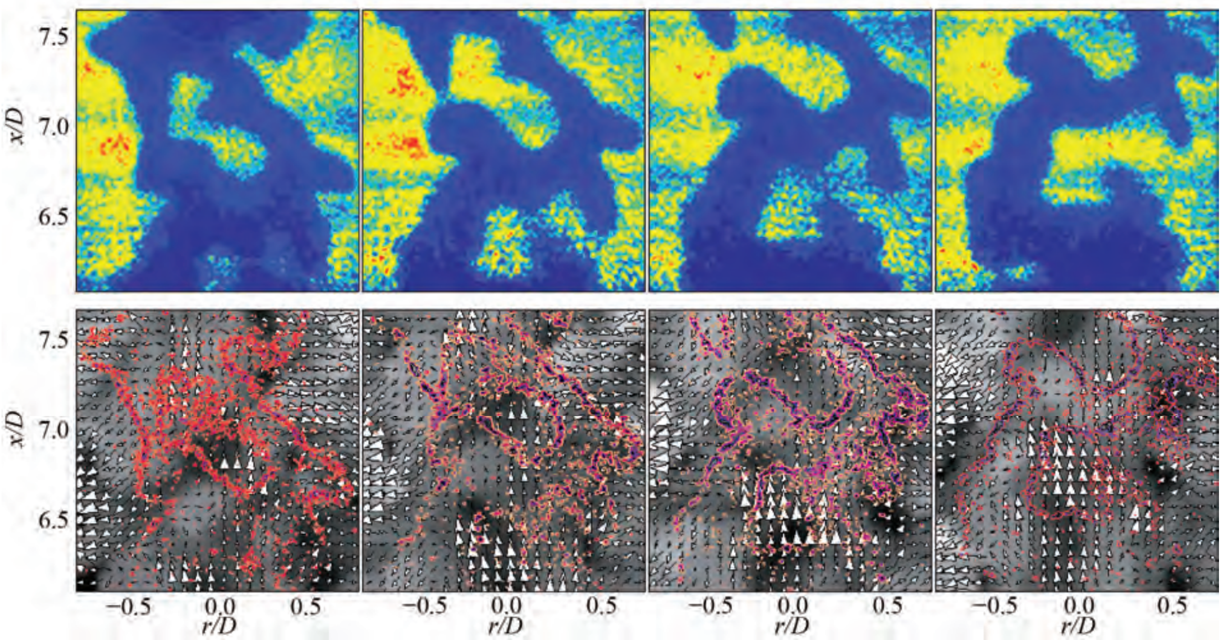

Fig. 18 PLIF images of OH (upper row) and CH and fluctuating velocity fields (lower row) for U_0 = 15 m/s, x/D_{in} = 7 and Re_λ = 173.1.

be disconnected. Between the disconnected unburned mixtures, the velocity field exhibits strong flow motion. At U_0 = 20 m/s (not shown here; see Johchi et al., 2015), the unburned mixture in the main jet frequently divides in two in the streamwise direction. The large scale turbulent structures in the downstream region are caused by Kelvin–Helmholtz instability of the shear layer. Consequently, large scale islands of unburned mixture are created and ejected into the downstream. Around the flame tip under the condition of high Reynolds number, the formation of fine scale unburned mixture islands was observed and its contribution to enhance the turbulent burning velocity was also investigated by statistically analyzing the local consumption rate (Johchi et al., 2015; Shimura et al., 2016). These high-repetition-rate and long-duration simultaneous measurement of PLIF and PIV will give more detailed information on dynamics of turbulent flames in the near future.

4. SUMMARY AND CONCLUDING REMARKS

In this paper, recent 3D DNS and advanced laser diagnostics of turbulence and turbulent combustion are summarized. The combination of various measurement techniques such as PLIF and PIV will give more detailed experimental data which have high accuracy enough to compare with DNS. The direct comparisons between experiment and DNS lead to deep insight into turbulence and turbulent combustion, which will contribute to the development of high efficient and low emission combustors.

ACKNOWLEDGMENT

The authors acknowledge the financial support of Grant-in-Aid for Scientific Research (A) (No.15206023), (S) (No.18106004), (B) (No.19360097), and (S) (No.23226005) of Japan Society for the Promotion of Science, by Grant-in-Aid for Young Scientists (S) (No.20676004) of Japan Society for the Promotion of Science, by Grant-in-Aid for Young Scientists (A) (No.16686011) of the Ministry of Education, Culture, Sports, Science and Technology, Japan and by the NEXT program (No. GR038) initiated by the Council for Science and Technology Policy (CSTP), Japan.

REFERENCES

Aoki, K., Shimura, M., Ogawa, S., Fukushima, N., Naka, Y., Nada, Y., Tanahashi, M. and Miyauchi, T., Short- and Long-term Dynamic Modes of Turbulent Swirling Premixed Flame in a Cuboid Combustor, Proc. Combust. Inst., Vol. 35, pp. 3209-3217, 2015.

Bell, J. B., Day, M. S., Shepherd, I. G., Johnson, M. R., Cheng, R. K., Grcar, J. F., Beckner, V. E. and Lijewski, M. J., Numerical Simulation of a Laboratory Scale Turbulent V-Flame, Proc. Natl. Acad. Sci., Vol. 102, pp. 10006-10011, 2005.

Bell, J. B., Day, M. S., Grcar, J. F., Lijewski, M. J., Driscoll, J. F. and Filatyev, S. A., Numerical Simulation of a Laboratory-Scale Turbulent Slot Flame, Proc. Combust. Inst., Vol. 31, pp. 1299-1307, 2007.

Chen, J. H., Hawkes, E. R., Sankaran, R., Mason, S. D. and Im, H. G., Direct Numerical Simulation of Ignition Front Propagation in a Constant Volume with Temperature Inhomogeneities I. Fundamental Analysis and Diagnostics, Combust. Flame, Vol. 145, pp. 128-144, 2006.

Del Alamo, J. C., Jimenez, J., Zandonade, P. and Moser, R. D., Self-similar Vortex Clusters in the Turbulent Logarithmic Region, J. Fluid Mech., Vol. 561, pp. 329-358, 2006.

Donbar, J. M., Driscoll, J. F. and Carter, C. D., Reaction Zone Structure in Turbulent Nonpremixed Jet Flames - from CH-OH PLIF Images, Combust. Flame., Vol. 122, No. 1-2, pp. 1-19, 2000.

Donbar, J. M., Driscoll, J. F. and Carter, C. D., Strain Rates Measured along the Wrinkled Flame Contour within Turbulent Non-Premixed Jet Flames, Combust. Flame., Vol. 125, No. 4, pp. 1239-1257, 2001.

Fukumoto, H., Seo, T., Shimura, M., Fukushima, N., Tanahashi, M. and Miyauchi, T., DNS Investigation on Autoignition and Flame Propagation in HCCI Combustion, J. Fluid Sci. Tech., Vol. 6, pp. 45-55, 2011.

Fukushima, N., Katayama, M., Naka, Y., Oobayashi, T., Shimura, M., Nada, Y., Tanahashi, M. and Miyauchi, T., Combustion Regime Classification of HCCI/PCCI Combustion using Lagrangian Fluid Particle Tracking, Proc. Combust. Inst., Vol. 35, pp. 3009-3017, 2015.

Fukushima, N., Shiono, H., Shimura, M., Yoshikawa, I., Tanahashi, M. and Miyauchi, T., Pressure Effects on Flame Structure in Turbulent V-Flame, Proc. 4th Asian Symp. Comput. Heat Transfer and Fluid Flow, 2013.

Hawkes, E. R., Sankaran, R., Chen, J. H., Kaiser, S. A. and Frank, J. H., An Analysis of Lower-Dimensional Approximations to the Scalar Dissipation Rate Using Direct Numerical Simulations of Plane Jet Flames, Proc. Combust. Inst., Vol. 32, pp. 1455-1463, 2009.

Hiraoka, K., Minamoto, Y., Shimura, M., Naka, Y., Fukushima, N. and Tanahashi, M., A Fractal Dynamic SGS Combustion Model for Large Eddy Simulation of Turbulent Premixed Flames, Combust. Sci. Technol., Vol. 188, pp. 1472-1495, 2016.

Hiraoka, K., Naka, Y., Shimura, M., Minamoto, Y., Fukushima, N., Tanahashi, M. and Miyauchi, T., Evaluations of SGS Combustion, Scalar Flux and Stress Models in a Turbulent Jet Premixed Flame, Flow Turb. Combust., Vol. 97, pp. 1147-1164, 2016.

Jimenez, J., Wray, A. A., Saffman, P. G. and Rogallo, R. S., The Structure of Intense Vorticity in Isotropic Turbulence, J. Fluid Mech., Vol. 255, pp. 65-90, 1993.

Johchi, A., Naka, Y., Shimura, M., Tanahashi, M. and Miyauchi, T., Investigation on Rapid Consumption of Fine Scale Unburned Mixture Islands in Turbulent Flame via 10 kHz Simultaneous CH-OH PLIF and SPIV, Proc. Combust. Inst., Vol. 35, No. 3, pp. 3663-3671, 2015.

Kaminski, C .F., Hult, J. and Alden, M., High Repetition Rate Planar Laser Induced Fluorescence of OH in a Turbulent Non-premixed Flame, Appl. Phys. B, Vol. 68, pp. 757-760, 1999.

Kang, S. J., Tanahashi, M. and Miyauchi, T., Elliptic Feature of Coherent Fine Scale Eddies in Turbulent Channel Flows, J. Mech. Sci. Technol., Vol. 20, pp. 262-270, 2006.

Knaus, D.A. and Gouldin, F.C., Measurements of Flamelet Orientations in Premixed Flames with Positive and Negative Markstein Numbers, Proc. Combust. Inst., Vol. 28, pp. 367-272, 2000.

Luo, K., Pitsch, H., Pai, M. G. and Desjardins, O., Direct Numerical Simulations and Analysis of Three-Dimensional n-Heptane Spray Flames in a Model Swirl Combustor, Proc. Combust. Inst., Vol. 33, pp. 2143-2152, 2011.

Minamoto, Y., Aoki, K., Tanahashi, M. and Swaminathan, N., DNS of Swirling Hydrogen-air Premixed Flame, Int. J. Hydrogen Energy, Vol. 40, pp. 13604-13620, 2015.

Minamoto, Y., Fukushima, N., Tanahashi, M., Miyauchi, T., Dunstan, T. and Swaminathan, N., Effect of Flow-Geometry on Turbulence-Scalar Interaction in Premixed Flames, Phys. Fluids, Vol. 23, pn.125107, 2011.

Miyata, E., Fukushima, N., Naka, Y., Shimura, M., Tanahashi, M. and Miyauchi, T, Direct Numerical Simulation of Micro Combustion in a Narrow Circular Channel with a Detailed Kinetic Mechanism, Proc. Combust. Inst., Vol. 35, pp. 3421-3427, 2015.

Naka, Y., Tomita, K., Shimura, M., Fukushima, N., Tanahashi, M. and Miyauchi, T., Quad-plane Stereoscopic PIV for Fine Scale Structure Measurements in Turbulence, Exp. Fluids, Vol. 57, No. 63, 20pp, 2016.

Peterson, B., Baum, E., Böhm, B. and Dreizler, A., Early Flame Propagation in a Spark-ignition Engine Measured with Quasi 4D-diagnostics, Proc. Combust. Inst., Vol. 35, pp. 3829-3837, 2015.

Poinsot, T. and Veynante, D., Theoretical and Numerical Combustion, Edwards, 2005.

Sankaran, R., Hawkes, E. R., Chen, J. H., Lu, T. and Law, C. K., Structure of a Spatially Developing Turbulent Lean Methane-Air Bunsen Flame, Proc. Combust. Inst., Vol. 31, pp. 1291-1298, 2007.

Schefer, R. W., Namazian, M., Filtopoulos, E. E. J. and Kelly, J., Temporal Evolution of Turbulence/Chemistry Interactions in Lifted, Turbulent-jet Flames, Proc. Combust. Inst., Vol. 25, pp. 1223-1231, 1994.

Shim, Y.-S., Fukushima, N., Shimura, M., Nada, Y., Tanahashi, M. and Miyauchi, T., Radical Fingering in Turbulent Premixed Flame Classified into Thin Reaction Zones, Proc. Combust. Inst., Vol. 34, pp. 1383-1391, 2013.

Shim, Y.-S., Shimura, M., Fukushima, N., Tanahashi, M. and Miyauchi, T., 3D Flame Structures in High Reynolds Number Turbulence, Proc. 22nd Int. Symp. Transport Phenomena, 2011.

Shimura, M., Ueda, T., Choi, G.-M., Tanahashi, M. and Miyauchi, T., Simultaneous Dual-plane CH PLIF, Single-plane OH PLIF and Dual-plane Stereoscopic PIV Measurements in Methane-air Turbulent Premixed Flames, Proc. Combust. Inst., Vol. 33, pp. 775-782, 2011.

Shimura, M., Yamawaki, K., Fukushima, N., Shim, Y.-S., Nada, Y., Tanahashi, M. and Miyauchi, T., Flame and Eddy Structures in Hydrogen-Air Turbulent Jet Premixed Flame, J. Turbulence, Vol. 13, N42, 2012.

Shimura, M., Johchi, A. and Tanahashi, M., Consumption Rate Characteristics of a Fine-scale Unburnt Mixture in a Turbulent Jet Premixed Flame by High Repetition Rate PLIF and SPIV, J. Therm. Sci. Tech., Vol. 11, No. 3, p. JTST0047, 2016.

Tanahashi, M., Miyauchi, T. and Ikeda, J., Identification of Coherent Fine Scale Structure in Turbulence, IUTAM Symp Simulation and Identification of Organized Structures in Flows, Vol. 52, pp. 131-140, 1997.

Tanahashi, M., Nada, Y., Fujimura, N. and Miyauchi, T., Fine Scale Structure of H_2-air Turbulent Premixed Flames, 1st Int. Symp. Turbulence Shear Flow Phenomena, Banerjee, S. and Eaton, J. Eds, pp. 59-64, 1999.

Tanahashi, M., Fujimura, M. and Miyauchi, T., Coherent Fine Scale Eddies in Turbulent Premixed Flames, Proc. Combust. Inst., Vol. 28, pp. 529-535, 2000.

Tanahashi, M., Iwase, S. and Miyauchi, T., Appearance and Alignment with Strain Rate of Coherent Fine Scale Eddies in Turbulent Mixing Layer, J. Turbulence, Vol. 2 No. 6, 2001.

Tanahashi, M., Nada, Y., Ito, Y. and Miyauchi, T., Local Flame Structure in the Well-Stirred Reactor Regime, Proc. Combust. Inst., Vol. 29, pp. 2041-2049, 2002.

Tanahashi, M., Kang, S. J., Miyamoto, T., Shiokawa, S. and Miyauchi, T., Scaling Law of Coherent Fine Scale Eddies in Turbulent Channel Flows up to $Re_\tau = 800$, Int. J. Heat Fluid Flow, Vol. 25, pp. 331-340, 2004a.

Tanahashi, M., Fukuchi, Y., Choi, G.-M., Fukuzato, K. and Miyauchi, T., The Time-resolved Stereoscopic Digital Particle Image Velocimetry up to 26.7 kHz, Proc 12th Int. Symp. Appli. Laser Tech. Fluid Mech., 2004b.

Tanahashi, M., Murakami, S., Choi, G.-M., Fukuchi, Y. and Miyauchi, T., Simultaneous CH-OH PLIF and Stereoscopic PIV Measurements of Turbulent Premixed Flames, Proc. Combust. Inst., Vol. 30, pp. 1665-1672, 2005.

Tanahashi, M., Hirayama, T., Taka, S. and Miyauchi, T., Measurement of Fine Scale Structure in Turbulence by Time-resolved Dual-plane Stereoscopic PIV, Int. J. Heat Fluid Flow, Vol. 29, pp. 792-802, 2008a.

Tanahashi, M., Taka, S., Shimura, M. and Miyauchi, T., CH Double-pulsed PLIF Measurement in Turbulent Premixed Flame, Exp. Fluids, Vol. 45, pp. 323-332, 2008b.

Tanahashi, M., Taka, S., Hirayama, T., Minamoto, Y. and Miyauchi, T., Local Burning Velocity Measurements in Turbulent Jet Premixed Flame by Simultaneous CH DPPLIF/OH PLIF and Stereoscopic PIV, Proc. 14th Int.

Symp. Appli. Laser Tech. Fluid Mech., 2008c.

Tanaka, S., Shimura, M., Fukushima, N., Tanahashi, M. and Miyauchi, T., DNS of Turbulent Swirling Premixed Flame in a Micro Gas Turbine Combustor, Proc. Combust. Inst., Vol. 33, pp. 3293-3300, 2011.

Trunk, P. J., Boxx, I., Heeger, C., Meier, W., Böhm, B. and Dreizler, A., Premixed Flame Propagation in Turbulent Flow by Means of Stereoscopic PIV and Dual-plane OH-PLIF at Sustained kHz Repetition Rates, Proc. Combust. Inst., Vol. 34, pp. 3565-3572, 2013.

Ueda, T., Shimura, M., Tanahashi, M. and Miyauchi, T., Measurement of Three-Dimensional Flame Structure by Combined Laser Diagnostics, J. Mech. Sci. Tech., Vol. 23, pp. 1813-1820, 2009.

Wang, H., Luo, K., Lu, S. and Fan, J., Direct Numerical Simulation and Analysis of a Hydrogen/Air Swirling Premixed Flame in a Micro Combustor, Int. J. Hydrogen Energy, Vol. 36, pp. 13838-13849, 2011.

Wang, Y., Tanahashi, M. and Miyauchi, T., Coherent Fine Scale Eddies in Turbulent Transition of Spatially-Developing Mixing Layer, Int. J. Heat Fluid Flow, Vol. 28, pp. 1280-1290, 2007.

Watson, K. A., Lyons, K. M., Carter, C. D. and Donbar, J. M., Simultaneous Two-shot CH Planar Laser Induced Fluorescence and Particle Image Velocimetry Measurements in Lifted CH_4/Air Diffusion Flames, Proc. Combust. Inst., Vol. 29, pp. 1905-1912, 2002.

Yenerdag, B., Fukushima, N., Shimura, M., Tanahashi, M. and Miyauchi, T., Turbulence-Flame Interaction and Fractal Characteristics of H_2-Air Premixed Flame under Pressure Rising Condition, Proc. Combust. Inst., Vol. 35, pp. 1277-1285, 2015.

Yoo, C.S., Luo, Z., Lu, T., Kim, H. and Chen, J.H., A DNS Study of Ignition Characteristics of a Lean Iso-octane/Air Mixture under HCCI and SACI Conditions, Proc. Combust. Inst., Vol. 34, pp. 2985-2993, 2013.

Zhang, H., Hawkes, E. R., Chen, J. H. and Kook, S., A Numerical Study of the Autoignition of Dimethyl Ether with Temperature Inhomogeneities, Proc. Combust. Inst., Vol. 34, pp. 803-812, 2013.